PIN6 auxin transporter at endoplasmic reticulum and plasma membrane mediates auxin homeostasis and organogenesis in Arabidopsis

Sibu Simon[1,2,3], Petr Skůpa[4], Tom Viaene[2], Marta Zwiewka[3], Ricardo Tejos[2], Petr Klíma[4], Mária Čarná[4], Jakub Rolčík[5], Riet De Rycke[2,6], Ignacio Moreno[7], Petre I. Dobrev[4], Ariel Orellana[7], Eva Zažímalová[4] and Jiří Friml[1]

[1]Institute of Science and Technology Austria (IST Austria), 3400, Klosterneuburg, Austria

[2]Department of Plant Systems Biology, VIB and Department of Plant Biotechnology and Biotechnology, Ghent University, 9052 Ghent, Belgium

[3]CEITEC - Central European Institute of Technology, Masaryk University, 625 00 Brno, Czech Republic

[4]Institute of Experimental Botany, Academy of Sciences of the Czech Republic, Rozvojová 263, 16502 Prague 6, Czech Republic

[5]Laboratory of Growth regulators, Centre of the Region Haná for Biotechnological and Agricultural Research, Faculty of Science, Palacký University, 78371 Olomouc, Czech Republic

[6]Inflammation Research Center, VIB 9052 Ghent, Belgium

[7]Center for Genome Regulation, Center of Plant Biotechnology, Facultad de Ciencias Biologicas, Universidad Andres Bello, Santiago, Chile

Author for correspondence:

Prof. Jiri Friml

Tel: +43 (0)2243 9000 5401; E-mail: jiri.friml@ist.ac.at

Total word count (excluding summary references and legends): 4111

Summary: 197

Introduction: 514

Materials and Method: 919

Results: 1880

Discussion: 755

Acknowledgement: 53

Number of figures: 4 (Figs 1&4 in colour)

No. of Tables: 0

Supporting information: 4 figures; 1 table

Summary

- Plant development mediated by the phytohormone auxin depends on tightly controlled cellular auxin levels at its target tissue that are largely established by the by inter- and intracellular auxin transport mediated by PIN auxin transporters. Among the eight members of the Arabidopsis PIN family, PIN6 is the least characterized candidate.

- In this study we generated functional, fluorescent protein-tagged PIN6 proteins and performed comprehensive analysis of their subcellular localization and also performed a detailed functional characterization of PIN6 and its developmental roles.

- The localization study of PIN6 revealed a dual localization at the plasma membrane (PM) and endoplasmic reticulum (ER). Transport and metabolic profiling assays in cultured cells and Arabidopsis strongly suggest that PIN6 mediates both auxin transport across the PM and intracellular auxin homeostasis, including the regulation of free auxin and auxin conjugates levels. As evidenced by the loss- and gain-of-function analysis, the complex function of PIN6 in auxin transport and homeostasis is required for auxin distribution during lateral and adventitious root organogenesis and for progression of these developmental processes.

- These results illustrate a unique position of PIN6 within the family of PIN auxin transporters and further add complexity to the developmentally crucial process of auxin transport.

Introduction

Auxin is a major player among plant hormones and its pivotal role in various plant growth and developmental events has been demonstrated by decades of research (reviewed in: Benjamins and Scheres, 2008; Mockaitis and Estelle, 2008; Vanneste and Friml, 2009). Among plant hormones, auxin is well known for its property that it is transported throughout plant tissues in a directional, regulated manner (reviewed in: Kramer and Bennett, 2006; Blakeslee *et al.*, 2006; Grunewald and Friml, 2010). Moreover, the transport-assisted auxin concentration maxima and gradients at the target tissue/cell types have a crucial role in mediating auxin-mediated developmental events (reviewed in Adamowski and Friml, 2015).

The transport of auxin across the plasma membrane (PM) is mediated by at least three protein families, namely the amino acid permease-like AUXIN1 (AUX1)/LIKE AUX1 (LAX) import mediators, the plant-specific PIN-FORMED (PIN) auxin transport mediators, and the plant orthologues of the mammalian ATP-binding cassette subfamily B (ABCB)-type transporters (Bennett *et al.*, 1996; Geisler *et al*, 2005; Petrášek *et al.*, 2006; reviewed in Petrášek and Friml, 2009). In Arabidopsis, the PIN family consists of 8 members; PIN1-4 and 7 localize at the PM to mediate intercellular auxin transport (reviewed in: Petrášek and Friml, 2009; Zažímalová *et al.*, 2010; Forestan and Varotto, 2012). In contrast, PIN5 and PIN8, characterized by a short middle cytosolic hydrophilic loop, still having auxin transport activity, localize in cells of their endogenous expression domain to the endoplasmic reticulum (ER) and were proposed to have a function in regulating cellular auxin homeostasis (Mravec *et al.*, 2009; Dal Bosco *et al.*, 2012; Ding *et al.*, 2012).

PIN6 is another member of the PIN family of auxin transporters, which has been partially characterized. The PIN6 gain-of-function phenotype in *Arabidopsis thaliana* revealed a role for PIN6 during lateral root development (Cazzonelli *et al.*, 2013), while also a role during

4

leaf vasculature development and nectar secretion has been reported (Sawchuk *et al*., 2013; Bender *et al*., 2013). In addition to lateral roots, detailed expression study reported their expression in primary root vasculature, cotyledons, cauline leaves, floral stem, sepels and in siliques (Nisar *et al*., 2014). Despite the indication of a subcellular localization at the ER when expressed heterologously in tobacco BY-2 cells (Mravec *et al*., 2009) or in Arabidopsis (Sawchuk *et al*., 2013; Bender *et al*., 2013), it is noticeable that the middle hydrophilic loop of PIN6 has more than 250 amino acid residues but the 'short' ER-localized PINs; i.e. in PIN5 and PIN8 it is less than 50 amino acids in length (Bennett et al., 2014). Moreover, most of the Ser/Thr phosphorylation sites, which are known to be important for the polar localization at the PM of 'long' PINs (Huang *et al*., 2010; Zhang *et al*., 2010), are also present in the PIN6 hydrophilic loop, suggesting that PIN6 may have a unique role, different from the previously described 'short' and 'long' PINs.

Here, we characterized PIN6 with respect to its evolutionary origin, localization and function in auxin transport and metabolism along with PIN6 developmental roles, revealing unique properties of PIN6 with a dual role both at the ER and the PM.

Materials and Methods

Plant material and DNA constructs

For all experiments, we used *Arabidopsis thaliana* ecotype Columbia (Col-0). The insertion mutant we used was *pin6-2* (Bender *et al*., 2013). Other transgenic lines used were *PIN6:PIN6-GFP* (Sawchuk *et al*., 2013), PIN6 overexpressor: *PIN6-OE#14; DR5:GUS/PIN6-OE#14* (Cazzonelli *et al*., 2013) and *DR5:GUS* (Ulmasov *et al*., 1997). The stably transformed, tobacco BY-2-derived cell line *GVG-PIN6* (Petrášek *et al*., 2006) was used for transport and metabolic

assays. The *35S:PIN6-GFP* plasmids were prepared by the Gateway cloning technology (www.invitrogen.com). The eGFP sequence was inserted in three different positions of the PIN6 coding sequence by overlap PCR and these three independent recombinants were cloned into pDNR221. The expression clone was prepared by an LR reaction between entry clone and expression vector pB7WG2.0. The resulting constructs were transformed into Arabidopsis (Col-0) plants by floral dipping in *Agrobacterium tumefaciens* liquid cultures (Clough *et al*., 1998). The primers used for the preparation of these constructs included in Supporting Information Table S1.

Growth conditions

Arabidopsis seeds were sterilized with chlorine gas and stratified at 4 ℃ for 2 days in the dark. Seedlings were grown vertically on half-strength Murashige and Skoog (MS) medium supplemented with 1% sucrose and respective nutrients. Plants were grown under long-day conditions at 21 ℃ in growth chambers unless stated otherwise. *GVG-PIN6* tobacco cells were grown as described earlier (Petrášek *et al*., 2006) in presence of 40 μg/L hygromycin and PIN6 expression was induced by the addition of 1 μM dexamethasone (DEX) for 48 h.

Pharmacological and hormonal treatments

ER-tracker dye (Invitrogen) was used in a 1:1000 dilution and the seedlings were treated for 30 minutes in AM liquid medium. BFA (Invitrogen) was used in a final concentration of 25 μM in dimethylsulfoxide (DMSO) stock solution. Seedlings were treated in AM liquid medium for 30 minutes. FM4-64 (Invitrogen) was dissolved in water and the seedlings were labelled with 4 μM FM4-64 for 5 min in MS liquid medium on ice, washed in MS liquid medium and observed immediately. Indole-3-acetic acid (IAA, Sigma-Aldrich) stock solution was prepared in ethanol

and plates were prepared with the concentrations mentioned. GUS staining was performed as described earlier (Benková *et al*., 2003).

Microscopy

A Zeiss LSM 710 confocal microscope was used for GFP, FM4-64 and DII-VENUS observations in Arabidopsis roots. The same confocal microscope was used also for all immunolocalization images. GUS stained root tips were observed by an Olympus BX53 microscope and images were taken using an Olympus DP26 camera with the help of Olympus cellSens Entry software. Lateral and adventitious root densities were measured by counting the number of lateral and adventitious roots under a Leica EZ2 optical microscope.

Phenotype analysis

For lateral root density measurements, seedlings were grown for 7 days as mentioned above. Each seedling was marked and plates were scanned on a flat-bed scanner to measure the primary root length by using imageJ (http://rsb.info.nih.gov/ij/). Lateral roots on each seedling were counted and the lateral root density was expressed in relation to the primary root length value. To measure the auxin effect on lateral root development, seedlings were grown vertically for 4 days, and then transferred to plates containing the necessary concentration of auxin and grown for an additional 4 days. Then, the lateral root density was measured as described above. The adventitious root density (Sukumar *et al*., 2003) and the lateral root primordia density (Malamy *et al*., 1997) were measured as previously described.

Auxin transport and auxin metabolic profiling assays

For yeast assays, microsomal fractions were prepared from yeast cells as previously described (Liang and Sze, 1998). Yeast microsomes obtained from the fractionations were used to

perform uptake assays. The auxin transport assay in tobacco BY-2 cells was performed as described earlier (Petrášek *et al*., 2006). Auxin measurements and auxin metabolic profiling were done as described in Mravec *et al*., (2009) and Simon *et al*. (2014).

Localization assays

Whole-mount immunolocalizations on Arabidopsis roots were performed as described (Sauer *et al*., 2006). Antibodies were diluted as follows: rabbit anti-PIN1 (1:1000) (Robert *et al*., 2010), rabbit anti-PIN2 (1:1000) (Wisniewska *et al*., 2006), rabbit anti-SEC21 (1:1000; Agrisera AS08 327), rabbit anti-BIP2 (1:200; Agrisera AS09 481), rabbit anti-ARF (1:600; Agrisera AS08 325), mouse anti-GFP (1:600; Sigma G6539), Cy3-conjugated secondary anti-rabbit (1:600; Sigma C2306) and Alexa Fluor 488 conjugated secondary anti-mouse (1:600; Invitogen A11029). Anti-GFP immunogold labelling method was adopted from Xu et al. (2014) using anti-GFP antibodies. Biolistic transient expression of genes in tobacco BY-2 cells was performed as described in Robert et al., 2011.

Membrane fraction isolation and western blotting

Membrane fractions were isolated from whole seedlings as described previously (Abas and Luschnig, 2010). The proteins were detected by western blot with mouse anti GFP primary antibody (1:3000; Sigma Aldrich) and subsequently with anti-mouse HRP conjugated antibody (1:10000; Sigma Aldrich).

Phylogenetic reconstruction

The phylogenetic tree showing the relationship between PIN proteins was constructed from four different angiosperm species: the basal angiosperm *Amborella trichopoda*, the monocots rice (*Oryza sativa*) and *Brachypodium distachyon*, and the dicots tomato (*Solanum*

lycopersicon) and *Arabidopsis thaliana*. Protein sequences were retrieved through BLAST from GenBank. Protein sequences (with the highly divergent hydrophilic loop omitted) were aligned using ClustalW and manually checked. We used this alignment to reconstruct a neighbor joining (NJ) tree using the phylogeny.fr platform and bootstrap values from 1000 replicates were calculated (Dereeper *et al*., 2008; Dereeper *et al*., 2010; Guindon *et al*., 2010). Bootstrap support over 75% from NJ analyses were put on the branches. Lengths of the hydrophilic loops were estimated with the TMHMM Server v.2.0 and placed next to the taxa (in amino acids).

Results

Evolution of PIN6 proteins

PIN6 has always been the peculiar one among other Arabidopsis PIN proteins. None of the so far completely sequenced genomes of non-angiosperm plant species contains obvious sequences homologous to PIN6*,* suggesting that it is absent in plant groups outside angiosperms. Also, in contrast to all other PINs, many published phylogenies did not show any clear PIN6-like sequences in monocots (Carraro *et al*., 2012; Forestan *et al*., 2012, Viaene *et al*., 2013; Bennett et al., 2014, Clouse and Carraro, 2014). However, recently published trees show a close association between *AtPIN6* and respectively a few PIN-like transcriptome sequences from a fern species (*Microlepia* sp., Viaene *et al*., 2013) and a group of monoliphyte sequences (Bennett *et. al.*, 2014) Finally, it was recently suggested that the angiosperm PIN6 clade originated through reduction of a canonical, previously described as 'long', PIN protein, from which probably all land plant PIN proteins evolved and independently of other 'short' PIN proteins (Bennett et al., 2014). To highlight the phylogenetic position of *AtPIN6*, we reconstructed the PIN protein evolution using PIN-sequences from the basal angiosperm

9

Amborella, the monocots rice and *Brachypodium* and the dicots Arabidopsis and tomato (Supporting Information Fig. S1). We recovered all PIN sub-clades that have been identified in previously published PIN phylogenies. Again, PIN6-like sequences from Arabidopsis and tomato constitute a separate clade from all 'long' PINs. Also, we did not recover any clear monocot PIN6-like homolog, but a putative sequence from *Amborella* that could be PIN6-like, further emphasizing a history of recurrent gene loss.

Arabidopsis PIN6 shows a dual ER and PM localization

We designed three independent PIN6-GFP fusion lines by inserting *GFP* in the *PIN6* coding sequence at three different positions: either between the transmembrane domains 3 and 4 (between two glycines at positions 96 and 97, line *35S:PIN6-GFP1*), within the hydrophilic loop (between proline 166 and glycine 167, i.e. line *35S:PIN6-GFP2*, and between two glycines at positions 252 and 253, i.e. line *35S:PIN6-GFP3*) (Fig. 1a). We placed these constructs under the control of the constitutive 35S promoter. We also included in the analysis the *PIN6:PIN6-GFP* line (Sawchuk *et al*., 2013), in which *GFP* is inserted at the end of the central hydrophilic loop and the construct is placed under the control of its native promoter (GFP4). Unlike the other two GFP fusion lines, the *35S:PIN6-GFP1* line showed wavy root seedling phenotype and short plant phenotypes corresponding with the already published data for the untagged PIN6 overexpressor (PIN6-OE#14) (Cazzonelli *et al*., 2013) and older seedlings developed significantly longer lateral root from root-shoot junction (Supporting Information Fig. S2a,b,c). Moreover, this construct rescued the partially open flower phenotype of the *pin6-2* knock-out mutant (Supporting Information Fig. S2d). Therefore, this functional PIN6-GFP1 fusion was used for further analysis.

In the *35S:PIN6-GFP1* line, PIN6 localized both at the PM and ER (Fig. 1b,c) and identical subcellular localizations were observed for the *PIN6:PIN6-GFP* line (Fig. 1d). Co-

10

localization study with specific subcellular markers, i.e. ER-tracker dye (ER) and the FM4-64 (PM), confirmed the dual localization of PIN6 in *PIN6:PIN6-GFP* line (Fig. 1e-g). We also conducted a co-localization analysis with the *35S:PIN6-GFP1* line. Although PIN6 largely co-localized with both the ER marker BIP2 and the PM marker FM4-64, it also showed a weak co-localization with Golgi and trans-Golgi network (TGN) markers Sec21 and ARF1, respectively (Fig. 1h, Supporting Information Fig. S3a-d). To address the possibility that the ER signal is not an artifact of the ectopically increased expression, we used a weakly expressing *35S:PIN6-GFP1* line and also this line showed ER signal (Supporting Information Fig. S3e). We also treated *35S:PIN6-GFP1* lines with the vesicle recycling inhibitor Brefeldin A (BFA) and observed intracellular aggregation of PIN6 in epidermal cells (Fig. 1j), as was shown for 'long', PM-localized, constitutively recycling PINs (Geldner *et al*., 2001), in contrast to the BFA-resistant localization of ER-localized PIN5 and PIN8 (Mravec *et al*., 2009; Ding *et al*., 2012). This provides an additional evidence that PIN6 is also a PM-localized protein undergoing constitutive recycling. As additional test for the PIN6 subcellular distribution, we transiently co-expressed *35S:PIN6-GFP* and *35S:PIN1-RFP* in tobacco BY-2 cells and observed internal ER signal only for PIN6-GFP whereas PIN1-RFP showed dominant PM localization, where it co-localized with PM-fraction of PIN6 (Supporting Information Fig. S3f). In the same way we co-expressed *35S:PIN6-GFP1* and the ER marker *35S:HDEL-RFP* and both markers showed perfect co-localization (Supporting Information Fig. S3g). Anti-GFP immunogold labeling on ultrathin sections from the *35S:PIN6-GFP1* primary roots confirmed the dual localization of PIN6 at both the ER and PM (Fig. 1i). Finally, to confirm that the PIN6-GFP1 is full length in all sub-cellular compartments, microsomal membrane fractions were isolated from *35S:PIN6-GFP1* plants and performed western blotting using anti-GFP antibody. We observed only 89 kDa single protein band in both the membrane fractions as well as intracellular fractions, similar

to the PIN1-GFP positive control, which is also showed a single band (94 kDa) whereas no protein was detected in Col-0 (Supporting Information Fig. S3i).

Since PIN6 showed not only ER but also PM localization, we analyzed whether PIN6 also shows an asymmetric polar localization within the cell. Therefore we analyzed the co-localization pattern of PIN6 with other polarly localized markers like PIN1 and PIN2. We found that in the *35S:PIN6-GFP1* line, both PIN1 and PIN2 co-localized with PIN6 in vasculature and epidermis, respectively (Fig. 1k, l). In the *PIN6:PIN6-GFP* line, in which PIN6 is expressed in the vasculature of the root meristem zone, PIN6 also co-localized with PIN1 (Supporting Information Fig. S3h). This suggests that the PM-residing portion of PIN6 can adopt different polar localizations and thus may assists in transporting auxin in the directional manner.

PIN6 is a functional auxin transporter

The auxin transport function of PIN6 was analysed by two independent methods. First, PIN6 was heterologously expressed in yeast and an isolated microsomal fraction was used to run an auxin uptake assay with radiolabelled IAA. Microsomal fractions from a yeast strain overexpressing PIN6 showed a higher retention of radioactivity, which is an indication that PIN6 recognizes IAA as a substrate (Fig. 2a). To characterize the PIN6-mediated auxin transport in more detail, we used tobacco BY-2 suspension cultured cells in which PIN6 was overexpressed under a glucocorticoid (dexamethasone)-inducible promoter (Petrášek *et al.*, 2006). Phenotypic analysis of tobacco BY-2 cells overexpressing PIN6 following dexamethasone induction showed a typical auxin starvation phenotype characterized by reduced frequency of cell divisions, pronounced cell elongation and increased amyloplast formation (Mravec et al., 2008; Petrášek *et al.*, 2006) consistent with presumable PIN6 activity in decreasing free intracellular auxin levels (Fig. 2b,c). To measure the PIN6-mediated auxin transport, we used two radiolabelled synthetic auxins, naphthalene-1-acetic acid and 2,4-

12

dichlorophenoxyacetic acid (NAA and 2,4-D, respectively). PIN6 overexpression resulted in a reduced retention of the radiolabeled NAA in tobacco BY-2 cells suggesting that PIN6 promoted efflux of NAA from BY-2 cells. The overall decrease in the NAA accumulation was sensitive to the known auxin efflux inhibitor 1-naphthylphthalamic acid (NPA) and the degree of NPA-dependent inhibition was roughly the same for both control and PIN6-overexpressing cells (Fig. 2d). Similar decrease in retention was observed for radiolabelled 2,4-D, suggesting that PIN6 also recognizes 2,4-D as a substrate for transport out of cells (Fig. 2e) as it was reported earlier for PIN7 (Petrášek *et al*., 2006). These results from tobacco cells show that PIN6 mediates auxin transport out of the cells, similarly to other PM-localized PIN proteins.

PIN6 is involved in regulating auxin homeostasis

Previously, the ER-localized PIN5 and PIN8 proteins were suggested to regulate auxin homeostasis and/or metabolism by mediating auxin transport between the cytoplasm and ER-lumen (Mravec *et al*., 2009; Ding *et al*., 2012). To address a potential role of PIN6 in the regulation of auxin homeostasis we analyzed tobacco BY-2 cells that conditionally overexpressed PIN6. PIN6-expressing tobacco BY-2 cells following 2.5 hour incubation with [^{3}H]-IAA retained more non-metabolized, free IAA in cells (Fig. 3a). Such IAA metabolic profile has not been observed for overexpression of any PIN transporter analyzed so far.

To confirm the observations from the metabolic profiling, we quantified the levels of IAA and two IAA metabolites, indole-3-acetyl-aspartate (IAAsp) and indole-3-acetyl-glutamate (IAGlu) in Arabidopsis PIN6-OE#14 and *pin6-2* knock-out lines using mass spectroscopy (Mravec *et al*., 2009). Both knock-out and overexpressor lines showed higher levels of free IAA in the root tips (Fig. 3b). In addition to that, PIN6-OE#14 also exhibited a slightly and consistently elevated level of IAAsp as it was shown earlier for transgenic lines overexpressing ER-localized PIN5 (Mravec et al., 2009).

13

Altogether, these results suggest a role of PIN6 in regulation of cellular auxin levels and homeostasis.

PIN6 mediated auxin homeostasis regulates lateral and adventitious root development

Next, we analyzed how the function of PIN6 in auxin transport and homeostasis is reflected in developmental processes. The PIN6 expression pattern (Benkova et al., 2003) and gain-of-function studies (Cazzonelli *et al*., 2013) clearly indicated role of PIN6 in lateral root development. Therefore, we monitored the expression of the auxin response marker *DR5:GUS* (Ulmasov *et al*., 1997) during this process in seedlings with changed PIN6 activity. We observed a reduced auxin response in PIN6 overexpression lines during initial stages of lateral root development but a slightly increased response at the tips of developed lateral roots after emergence. In contrast, the *pin6-2* knock-out mutant showed an elevated auxin response in all stages of lateral root development (Fig. 4a), suggesting that PIN6 gain- and loss-of-function lines have opposite effects on the auxin levels during the initial stages of lateral root organogenesis.

In line with the changes in auxin response, we observed defects in lateral root development. The PIN6 overexpressor lines showed a higher number of lateral root primordia than the wild type (WT) or *pin6-2* knock-out (Fig. 4c) but significantly reduced density of emerged lateral roots (Fig. 4b) suggesting that overexpression of *PIN6* leads to increased lateral root initiation but delayed lateral root emergence. Notably, exogenous auxin application was able to rescue the defect in emerged lateral roots in the PIN6 overexpression lines (Fig. 4d). This suggests that *PIN6* overexpression reduces the free auxin available for lateral root primordia progression, which can be circumvented by exogenous auxin supply.

Adventitious root formation from Arabidopsis hypocotyl is also an auxin-dependent process with clear analogies to lateral root development (reviewed in Bellini *et al*., 2014). Therefore, we tested a role of PIN6-mediated auxin homeostasis in this process. We detected the PIN6 expression at the boundaries of the primordium base during adventitious root formation (Fig.4e) similar to pattern observed in lateral root primordia (Benkova et al., 2003; Cazzonelli et al., 2013). During this analysis we also noticed a strong expression of PIN6 in the area of root-shoot junction (Supporting Information Fig. S4). To test the role of PIN6 on adventitious root development, we adopted the method of decapitating primary roots in order to promote adventitious root initiation as recently described (Sukumar *et al*., 2013). As in lateral root development, PIN6 overexpression resulted in a dramatic decrease in adventitious roots formation even after decapitation of the primary root. On the contrary, the *pin6-2* knock-out line developed more adventitious roots already in the intact plants and this number further increased after decapitation (Fig. 4f). Thus, the *pin6* gain- and loss-of-function show opposite effects on adventitious root formation. In summary, the expression and function analysis revealed a role of PIN6 besides lateral root also in adventitious root development.

Discussion

The amino acid sequence with its "intermediate" hydrophilic loop places PIN6 between "long", PM-localized and "short" ER-localized PIN variants (reviewed in Adamowski and Friml, 2015). Previous work has shown that PIN6 localizes to the ER in BY2 suspension cultured cells (Mravec *et al*., 2009) and Arabidopsis leaf vasculature (Sawchuk *et al*., 2013). Another study reported the localization of PIN6 in internal compartments in Arabidopsis nectary (Bender *et al*., 2013). A more recent study analyzed the role of the PIN hydrophilic loop in PIN localization and observed PM localization of PIN5 when its short hydrophilic loop was replaced with that

of PIN2 (Ganguly *et al.*, 2014). The same study also reported the PM localization of PIN5 in the *PIN2* expression domain.

Our study explicitly demonstrates the dual localization of PIN6 in all cell types analyzed. This means that PIN6 itself carries molecular cues necessary to be localized both on the PM or ER. The overall PIN6 localization pattern under native and 35S promoters appear slightly different because of the different strength of the signal and different cell types they are expressed. Nonetheless, in both cases, we see consistently both ER and PM signal whereas overexpression of PIN1 or other "classical" PM PIN proteins did not result in ER localization neither in BY-2 nor in Arabidopsis regardless of the level of expression (Petrasek et al., 2006; Mravec et al., 2009; Löfke et., 2013). To further support the PM presence of PIN6, the PIN6 transport characteristics are similar to those found for 'long' PINs (Petrášek *et al.*, 2006). It is also worth noting that characteristic tyrosine motif (TPNTY), which is missing in PIN5 and is believed to be the signal related to the PM trafficking (Mravec *et al.*, 2009), is intact in PIN6 and there is also little variation in the amino acid sequence around this motif.

The higher retention of radioactive IAA in PIN6 over expressed yeast microsomal fraction is not providing information about PIN6 mediated auxin transport direction but it indicates that IAA is a substrate for PIN6. The reduction of the 2,4-D accumulation after PIN6 induction suggests that 2,4-D is also a substrate for PIN6, which is not a unique property for AtPIN6 alone. Active efflux of 2,4-D was also enhanced after the inducible overexpression of other PINs in BY-2 cells especially in the case of AtPIN7 as published in Petrášek et al. 2006. It is also valid for other long PINs tested in our system (unpublished data). So part of PIN6 auxin transport characteristics is analogous to already characterized PM localized long PINs.

The auxin metabolic profile of BY-2 cells overexpressing PIN6 showed a higher short-term retention of the free IAA, which contradicts the auxin starvation phenotype after prolonged

PIN6 overexpression in BY-2 cells. Similarly, elevated free IAA was detected in the PIN6 overexpressor Arabidopsis roots but the initial stage of the lateral root development in the same line showed reduced of *DR5*-monitored auxin response and only slightly higher auxin response in the emerged lateral root tips. This observation may reflect a special property of PIN6 in regulating auxin homeostasis in a developmental stage-specific manner. It is plausible that PIN6 overexpression causes intracellular compartmentalization of free IAA with hard-to-predict consequences on the overall auxin metabolism and free IAA levels. Our study also observed minor localization of PIN6 at the Golgi and trans Golgi network compartments but would be worth to extend the localization study to other intracellular compartments, in particular the vacuole since a previous study identified free IAA and IAA metabolites in vacuoles isolated from Arabidopsis (Ranocha et al., 2013) The higher auxin response at the lateral root tip may be due to the contribution of the polarly, PM-localized PIN6. It is also possible that PIN6 may have a tissue-specific, preferentially either PM or ER localization. There is also a strong expression of PIN6 in the shoot-root junction, which may act as a "gate" for the auxin coming from the shoot and absence of this barrier could be the reason for the elevated auxin content in the *pin6* knock-out mutants. Considering the complex localization pattern and auxin transport and homeostasis roles of PIN6, in future it would be interesting to see them expressed specifically in different cell types to analyze the differential localization pattern and auxin content regulation in different cell types.

Taken together, these results demonstrate a dual, PM- and ER-based, subcellular distribution of the atypical auxin transporter PIN6 and suggest its complex role in the control of auxin transport and homeostasis during auxin-mediated development including the lateral and adventitious root organogenesis.

Acknowledgements

References

Abas L, Luschnig C. 2010. Maximum yields of microsomal-type membranes from small amounts of plant material without requiring ultracentrifugation. *Analytical Biochemistry* **401:** 217-227.

Adamowski M, Friml J. 2015. PIN-dependent auxin transport: action, regulation and evolution. *The Plant Cell* **27:** 20-32.

Bender RL, Fekete ML, Klinkenberg PM, Hampton M, Bauer B, Malecha M, Lindgren K, Maki JA, Perera M, Nikolau BJ *et al*. 2013. PIN6 is required for nectary auxin response and short stamen development. *Plant Journal* **74:** 893-904.

Bellini C, Pacurar DI, Perrone I. 2014. Adventitious roots and lateral roots: similarities and differences. *Annual Review of Plant Biology* **65:** 639-666

Benjamins R, Scheres B. 2008. Auxin: the looping star in plant development. *Annual Review of Plant Biology* **59:** 443-465.

Benková E, Michniewicz M, Sauer M, Teichmann T, Seifertová D, Jürgens G, Friml J. 2003. Local, efflux-dependent auxin gradients as a common module for plant organ formation. *Cell* **115:** 591-602.

Bennett MJ, Marchant A, Green HG, May ST, Ward SP, Millner PA, Walker AR, Schulz B, Feldmann KA. 1996. *Arabidopsis AUX1* gene: a permease-like regulator of root gravitropism. *Science* **273:** 948-950.

Bennett T, Brockington SF, Rothfels C, Graham SW, Stevenson D, Kutchan T, Rolf M, Thomas P, Wong G K-S, Leyser O, Glover BJ, Harrison CJ. 2014. Paralogous radiations of PIN proteins with multiple origins of noncanonical PIN structure. *Molecular Biology and Evolution* **31:** 2042-2060.

Blakeslee JJ, Peer WA, Murphy AS. 2005. Auxin transport. *Current Opinion in Plant Biology* **8:** 494-500.

Carraro N, Tisdale-Orr TE, Clouse RM, Knöller AS, Spicer R. 2012. Diversification and expression of the PIN, AUX/LAX, and ABCB families of putative auxin transporters in *Populus*. *Frontiers in Plant Science* **3:** 17.

Cazzonelli CI, Vanstraelen M, Simon S, Yin K, Carron-Arthur A, Nisar N, Tarle G, Cuttriss AJ, Searle IR, Benkova E *et al*. 2013. Role of the Arabidopsis PIN6 auxin transporter in auxin homeostasis and auxin-mediated development. *PLoS One* **8:** e70069.

Clough SJ, Bent AF. 1998. Floral dip: a simplified method for *Agrobacterium*-mediated transformation of *Arabidopsis thaliana*. *Plant Journal* **16:** 735-743.

Clouse RM, Carraro N. 2014. A novel phylogeny and morphological reconstruction of the *PIN* genes and first phylogeny of the ACC-oxidases (ACOs). *Frontiers in Plant Science* **5**: 296.

Dal Bosco C, Dovzhenko A, Liu X, Woerner N, Rensch T, Eismann M, Eimer S, Hegermann J, Paponov IA, Ruperti B *et al*. 2012. The endoplasmic reticulum localized PIN8 is a pollen-specific auxin carrier involved in intracellular auxin homeostasis. *Plant Journal* **71:** 860-870.

Dereeper A, Audic S, Claverie JM, Blanc G. 2010. BLAST-EXPLORER helps you building datasets for phylogenetic analysis. *BMC Evolutionary Biology* **10:** 8.

Dereeper A, Guignon V, Blanc G, Audic S, Buffet S, Chevenet F, Dufayard JF, Guindon S, Lefort V, Lescot M *et al*. 2008. Phylogeny.fr: robust phylogenetic analysis for the non-specialist. *Nucleic Acids Research* **36:** 465-469.

Ding Z, Wang B, Moreno I, Dupláková N, Simon S, Carraro N, Reemmer J, Pěnčik A, Chen X, Tejos R *et al*. 2012. ER-localized auxin transporter PIN8 regulates auxin homeostasis and male gametophyte development in *Arabidopsis*. *Nature Communications*. **3:** 941.

Forestan C, Varotto S. 2012. The role of PIN auxin efflux carriers in polar auxin transport and accumulation and their effect on shaping maize development. *Molecular Plant* **5:** 787-798.

Forestan C, Farinati S, Varotto S. 2012. The Maize PIN Gene Family of Auxin Transporters. *Frontiers in Plant Science* **3:** 16.

Ganguly A, Park M, Kesawat MS, Cho HT. 2014. Functional analysis of the hydrophilic loop in intracellular trafficking of *Arabidopsis* PIN-FORMED proteins. *The Plant Cell* **26:** 1570-1585.

Geisler M, Blakeslee JJ, Bouchard R, Lee OR, Vincenzetti V, Bandyopadhyay A, Titapiwatanakun B, Peer WA, Bailly A, Richards EL, Ejendal KF, Smith AP, Baroux C, Grossniklaus U, Muller A, Hrycyna CA, Dudler R, Murphy AS, Martinoia E. 2005. Cellular efflux of auxin catalyzed by the *Arabidopsis* MDR/PGP transporter AtPGP1. *Plant Journal* **44:** 170-194.

Geldner N, Friml J, Stierhof YD, Jürgens G, Palme K. 2001. Auxin transport inhibitors block PIN1 cycling and vesicle trafficking. *Nature* **413:** 425-428.

Grunewald W, Friml J. 2010. The march of the PINs: developmental plasticity by dynamic polar targeting in plant cells. *EMBO Journal* **29:** 2700-2714.

Guindon S, Dufayard JF, Lefort V, Anisimova M, Hordijk W, Gascuel O. 2010. New algorithms and methods to estimate maximum-likelihood phylogenies: assessing the performance of PhyML 3.0. *Systematic Biology* **59:** 307-321.

Huang F, Zago MK, Abas L, van Marion A, Galván-Ampudia CS, Offringa R. 2010. Phosphorylation of conserved PIN motifs directs *Arabidopsis* PIN1 polarity and auxin transport. *The Plant Cell* **22:** 1129-1142.

Kramer EM, Bennett MJ. 2006. Auxin transport: a field in flux. *Trends in Plant Science* **11:** 382-386.

Liang F, Sze H. 1998. A high-affinity Ca2+ pump, ECA1, from the endoplasmic reticulum is inhibited by cyclopiazonic acid but not by thapsigargin. *Plant Physiology* **118:** 817-825.

Löfke C, Zwiewka M, Heilmann I, Van Montagu MC, Teichmann T, Friml J. 2013. Asymmetric gibberellin signaling regulates vacuolar trafficking of PIN auxin transporters during root gravitropism. *Proceedings of National Academy of Sciences* **110:** 3627-3632.

Malamy JE, Benfey PN. 1997. Organization and cell differentiation in lateral roots of *Arabidopsis thaliana*. *Development* **124:** 33-44.

Mockaitis K, Estelle M. 2008. Auxin receptors and plant development: a new signaling paradigm. *Annual Review of Cell and Developmental Biology* **24:** 55-80.

Mravec J, Kubes M, Bielach A, Gaykova V, Petrášek J, Skůpa P, Chand S, Benková E, Zazímalová E, Friml J. 2008. Interaction of PIN and PGP transport mechanisms in auxin distribution-dependent development. *Development* **135**: 3345-3354.

Mravec J, Skůpa P, Bailly A, Hoyerová K, Krecek P, Bielach A, Petrášek J, Zhang J, Gaykova V, Stierhof YD *et al*. 2009. Subcellular homeostasis of phytohormone auxin is mediated by the ER-localized PIN5 transporter. *Nature* **459:** 1136-1140.

Nisar N, Cuttriss AJ, Pogson BJ, Cazonelli CI. 2014. The promoter of the Arabidopsis PIN6 transporter enabled strong expression in the vasculature of roots, leave, floral stems and reproductive organs. *Plant Signaling & Behavior* **9:** e27898.

Petrášek J, Friml J. 2009. Auxin transport routes in plant development. *Development* **136:** 2675-2688.

Petrášek J, Mravec J, Bouchard R, Blakeslee JJ, Abas M, Seifertova D, Wisniewska J, Tadele Z, Kubes M, Covanova M *et al*. 2006. PIN proteins perform a rate-limiting function in cellular auxin efflux. *Science* **312:** 914-918.

Ranocha P, Dima O, Nagy R, Felten J, Corratgé-Faillie C, Novák O, Morreel K, Lacombe B, Martinez Y, Pfrunder S *et al.* 2013. *Arabidopsis* WAT1 is a vacuolar auxin transport facilitator required for auxin homeostasis. *Nature Communications* **4:** 2625

Robert S, Kleine-Vehn J, Barbez E, Sauer M, Paciorek T, Baster P, Vanneste S, Zhang J, Simon S, Čovanová M *et al*. 2010. ABP1 mediates auxin inhibition of clathrin-dependent endocytosis in *Arabidopsis*. *Cell* **143:** 111-121.

Sauer M, Paciorek T, Benková E, Friml J. 2006. Immunocytochemical techniques for whole-mount *in situ* protein localization in plants. *Nature Protocols* **1:** 98-103.

Sawchuk MG, Edgar A, Scarpella E. 2013. Patterning of leaf vein networks by convergent auxin transport pathways. *PLoS Genetics* **9:** e1003294.

Simon S, Skůpa P, Dobrev PI, Petrášek J, Zažímalová E, Friml J. 2014. Analyzing the in vivo status of exogenously applied auxins: a HPLC-based method to characterize the intracellularly localized auxin transporters. *Methods in Molecular Biology* **1056:** 255-264.

Sukumar P, Maloney GS, Muday GK. 2013. Localized induction of the ATP-binding cassette B19 auxin transporter enhances adventitious root formation in Arabidopsis. *Plant Physiology* **162:** 1392-1405.

Ulmasov T, Murfett J, Hagen G, Guilfoyle TJ. 1997. Aux/IAA proteins repress expression of reporter genes containing natural and highly active synthetic auxin response elements. *The Plant Cell* **9:** 1963-1971.

Vanneste S, Friml J. 2009. Auxin: a trigger for change in plant development. *Cell* **136:** 1005-1016.

Viaene T, Delwiche CF, Rensing SA, Friml J. 2013. Origin and evolution of PIN auxin transporters in the green lineage. *Trends in Plant Science* **18:** 5-10.

Wisniewska J, Xu J, Seifertová D, Brewer PB, Ruzicka K, Bililou I, Rouquié D, Benková E, Scheres B, Friml J. 2006. Polar PIN localization directs auxin flow in plants. *Science* **312:** 883.

Xu T, Dai N, Chen J, Nagawa S, Cao M, Li H, Zhou Z, Chen X, De Rycke R, Rakusová H, Wang W, Jones AM, Friml J, Patterson SE, Bleecker AB, Yang Z. 2014. Cell surface ABP1-TMK auxin-sensing complex activates ROP GTPase signaling. *Science* **343:** 1025-1028.

Yang H, Murphy AS. 2009. Functional expression and characterization of Arabidopsis ABCA, AUX1 and PIN auxin transporters in *Schizosaccharomyces pombe*. *Plant Journal* **59:** 179-191.

Zažímalová E, Murphy AS, Yang H, Hoyerová K, Hosek P. 2010. Auxin transporters- why so many? *Cold Spring Harbor Perspectives in Biology* **2:** a001552.

Zhang J, Nodzynski T, Pencík A, Rolcík J, Friml J. 2010. PIN phosphorylation is sufficient to mediate PIN polarity and direct auxin transport. *Proceedings of National Academy of Sciences* **107:** 918-922.

Figure legends

Figure 1. PIN6 shows a dual localization at the ER and PM. (a) Schematic representation of *GFP* insertion positions in the PIN6 coding sequence. (b) Five-day-old *35S:PIN6-GFP1* primary root tip showing both the ER and PM PIN6-GFP1 localization pattern in the root tip. (c) Higher magnification image of *35S:PIN6-GFP1* primary root cortex cells. (d) Localization pattern of PIN6-GFP in *PIN6:PIN6-GFP* primary root tip vasculature tissue. (e) Co-localization of PIN6-GFP with ER-tracker dye. GFP signal (left panel), ER-tracker dye (middle panel), merged (right panel). (f) Co-localization of PIN6-GFP with PM-staining dye (FM4-64). GFP signal (left panel), FM4-64 (middle panel), merged (right panel). (g) Quantification of co-localization of PIN6-GFP with ER-tracker dye and FM4-64. Error bar represent standard deviation (n=10 regions). (h) Quantification of co-localization of PIN6-GFP1 with ER marker BIP2, PM marker FM4-64, TGN marker ARF1 and Golgi marker Sec21. Error bar represent standard deviation (n=10 regions). (i) Anti-GFP immunogold labelling of *35S:PIN6-GFP1* root ultrathin section. The arrows show ER and PM labels. (j) PIN6-GFP1 after BFA treatment (arrows) in PIN6-GFP1 lines. (k) Co-localization of PIN6-GFP with the PIN1 basal polar marker in root vasculature. PIN6-GFP1 signal (left panel), PIN1 (middle panel), merged (right panel). (l) Co-localization of PIN6-GFP1 with the PIN2 apical polar marker in root epidermis. PIN6-GFP1 signal (left panel), PIN2 (middle panel), merged (right panel). Scale bars: 100 µm for (b); 5 µm for (c,d,e,f,j,k,l); 2 µm for (i).

Figure 2. PIN6 is a functional auxin transporter. (a) Radiolabelled IAA retention assay in a PIN6-overexpressing yeast microsomal fraction. Radioactivity is expressed as disintegrations per minute (dpm). Error bar represent standard deviation (n=3) (b) PIN6 overexpression phenotype of tobacco BY-2 suspension grown cells. Image shows a clear phenotypic change between WT (wild type, BY-2) and uninduced and PIN6-induced cells. (c) Graph representing

the PIN6 overexpression phenotype in terms of cell length and diameter in comparison of tobacco BY-2 cells conditionally expressing PIN6. (d) Accumulation of radiolabelled NAA as approximation of the active auxin efflux in both PIN6 induced and uninduced BY-2 cells. 1-Naphthylphthalamic acid (NPA) was used as an inhibitor of the auxin efflux. (e) Accumulation of radiolabelled 2,4-D in both PIN6 induced and uninduced BY-2 cells. Graph representing two independent (biological) experiments. Error bars show standard deviation (technical repetitions, n=3); if not visible, they fall into symbols.

Figure 3. PIN6 mediates auxin metabolism. (a) Comparison of IAA metabolic profiles between PIN6-overexpressing (induced) and uninduced tobacco BY-2 cells. Radiolabelled [^{3}H]-IAA, incubation time 2.5 h. PIN6 overexpression leads to a higher free IAA retention (three repetitions with the same result). (b) Quantification of free IAA and IAA metabolites IAAsp and IAGlu in PIN6 overexpression and *pin6-2* Arabidopsis root tips. Error bars represent standard deviation (n=3).

Figure 4. PIN6 mediates auxin-dependent lateral and adventitious root development. (a) Effect of PIN6 overexpression and knock-out on auxin response during lateral root development as monitored by the *DR5:GUS* signal. The image shows emerged lateral roots and two earlier stages of the lateral root development (from right to left). (b) Graph showing the emerged lateral roots of 8-day-old PIN6 overexpression and knock-out lines. LR, lateral roots, three independent experiments (n=15). (c) Total lateral root primordia density (calculating all stages of primordia development) in control (Col-0), PIN6 overexpression (PIN6-OE#14) and knock-out (*pin6-2*) lines, three repeats (n=15). (d) Effect of different concentrations of exogenously applied auxin on lateral root number in PIN6-OE#14 and *pin6-2* lines expressed as a percentage of non-treated (100%) in each line (n-15). (e) *PIN6:GUS* expression during adventitious root development is shown in stages of root initiation and emergence. (f) Effect of PIN6

overexpression and knock-out in adventitious root development. The graph shows both intact and primary root-decapitated variants of seedlings and the effect on adventitious root formation, as a proportion of intact Col-0 (100%) (n=15). Asterisks indicate the significance (Student's t-test) between control and experimental plants: *, $P < 0.05$; **, $P < 0.01$. #, $P < 0.05$ intact plants (h).

Supporting Information

Figure S1. Cladogram showing the evolution of PIN proteins.

Figure S2. Functionality of the *35S:PIN6-GFP1* construct. (a) Wavy root phenotype of 4-days-old PIN6-OE and *35S:PIN6-GFP1* seedlings. (b) Phenotype (root emerging from shoot-root junction) of 12-days-old PIN6-OE and *35S:PIN6-GFP1* seedlings. (c) Comparison of the phenotype of 4-week old *35S:PIN6* and *35S:PIN6-GFP1* seedlings with WT (Col-0). (d) Rescue of the partially closed flower phenotype of the *pin6-2* knock-out line by the *35S:PIN6-GFP1* construct.

Figure S3. PIN6 co-localization study with different markers. *35S:PIN6-GFP1* co-localization with (a) FM4-64, (b) BIP2, (c) ARF1, (d) Sec21. (e) PIN6-GFP expression pattern in a weak *35S:PIN6-GFP1* line. Arrow mark showing the possible ER signal. (f) Co-localization of *35S:PIN6-GFP1* and *35S:PIN1-RFP* constructs in transiently transfected BY-2 cells. (g) Co-localization of *35S:PIN6-GFP1* and *35S:HDEL-RFP* constructs in BY-2 cells. (h) *PIN6:PIN6-GFP* co-localization with the PIN1 polarity marker. Left panels: PIN6, middle panels: PIN1, right panels: merged. (i) Western blot of microsomal fractions isolated from the *35S:PIN6-GFP1* plants using anti-GFP antibody. Both intracellular and membrane fractions shows a

single band of PIN6-GFP1 89 kDa (arrow). Positive control PIN1-GFP also showing single band of protein with 94 kDa, which is absent in Col-0.

Figure S4. *PIN6:GUS* expression in shoot-root junction. Expression of PIN6 in root shoot junction.

Table S1. Primer sequences used for the preparation of PIN6-GFP constructs through overlap PCR

Figure 1

Figure 2

(a) [³H]-IAA retention (yeast)

PIN6 overexpression BY-2 phenotype

(b) WT

PIN6 induced

PIN6 uninduced

(c)
- WT
- PIN6 uninduced
- PIN6 induced

(d) [³H]-NAA retention (BY-2)
- □ PIN6 uninduced + NPA
- ■ PIN6 induced +NPA
- ○ PIN6 uninduced
- ● PIN6 induced

(e) [³H]-2,4-D retention (BY-2)
- ○ PIN6 uninduced
- ● PIN6 induced

Figure 3

(a) IAA metabolic profile in BY-2

PIN6 induced
PIN6 uninduced

IAA peak

Retention time

(b) IAA and IAA conjugate quantification in Arabidopsis

fmol/RT

Col 0   PIN6-OE   *pin6-2*

IAA
IAAsp
IAGlu

Figure 4

(a) DR5:GUS signal in lateral root

(b) Emerged lateral root density

(c) Total lateral root primordia (all stages)

(d) Emerged lateral root density (percentage)

(e) PIN6:GUS signal in adventitious root

(f) Emerged adventitious root (percentage)

Figure S1

PIN5-like (42-119 AA)

AmboPIN5
AtPIN5
OsPIN5a
BdPIN5a
OsPIN5c
BdPIN5c
OsPIN5b
BdPIN5b
SlPIN5b
SlPIN5

93
100
100
99
98
81
99
82

OsPIN9
BdPIN9
100

PIN8-like (59-113 AA)

AmboPIN8a
AmboPIN8b
SlPIN8
AtPIN8
OsPIN8
BdPIN8

100
100
100
100
100
93

PIN6-like (131-297AA)

AmboPIN6
AtPIN6
SlPIN6
100

BdPIN10b
OsPIN10b
OsPIN10a
BdPIN10a
98
94
92

PIN1-like (275-283 AA)

BdPIN1c
OsPIN1c
OsPIN1d
AmboPIN2
OsPIN2
BdPIN2
AtPIN2
SlPIN2
AmboPIN3
SlPIN4
SlPIN3
AtPIN4
AtPIN3
AtPIN7
AtPIN1
SlPIN1
BdPIN1b
OsPIN1b
OsPIN1a
BdPIN1a
AmboPIN1b
AmboPIN1a
SlPIN1c
SlPIN1b

100
100
100
100
96
87
79
100
100
96
100
100
96
100
60
99

Ambo: Amborella trichopoda(basal angiosperm)
Os: Oryza sativa (monocot)
Bd: Brachypodium distachyon (monocot)
At: Arabidopsis thaliana (eudicot)
Sl: Solanum lycopersicon (eudicot)

Figure S2

(a) PIN6-OE   35S:PIN6-GFP1

(b) Col-0   PIN6-OE   35S:PIN6-GFP

(c) Col 0   35S:PIN6   35S:PIN6-GFP1

(d) Col-0   pin6-2   pin6-2/35S:PIN6-GFP1

Figure S3

(a) *35S:PIN6-GFP1* + FM4-64

(b) *35S:PIN6-GFP1* + BIP2

(c) *35S:PIN6-GFP1* + ARF1

(d) *35S:PIN6-GFP1* + Sec21

(e) *35S:PIN6-GFP1* (weak)

(f) *35S:PIN6-GFP1* + *35S:PIN1-RFP*

(g) *35S:PIN6-GFP1* + *35S:HDEL-RFP*

(h) *PIN6:PIN6-GFP1* + PIN1

(i)

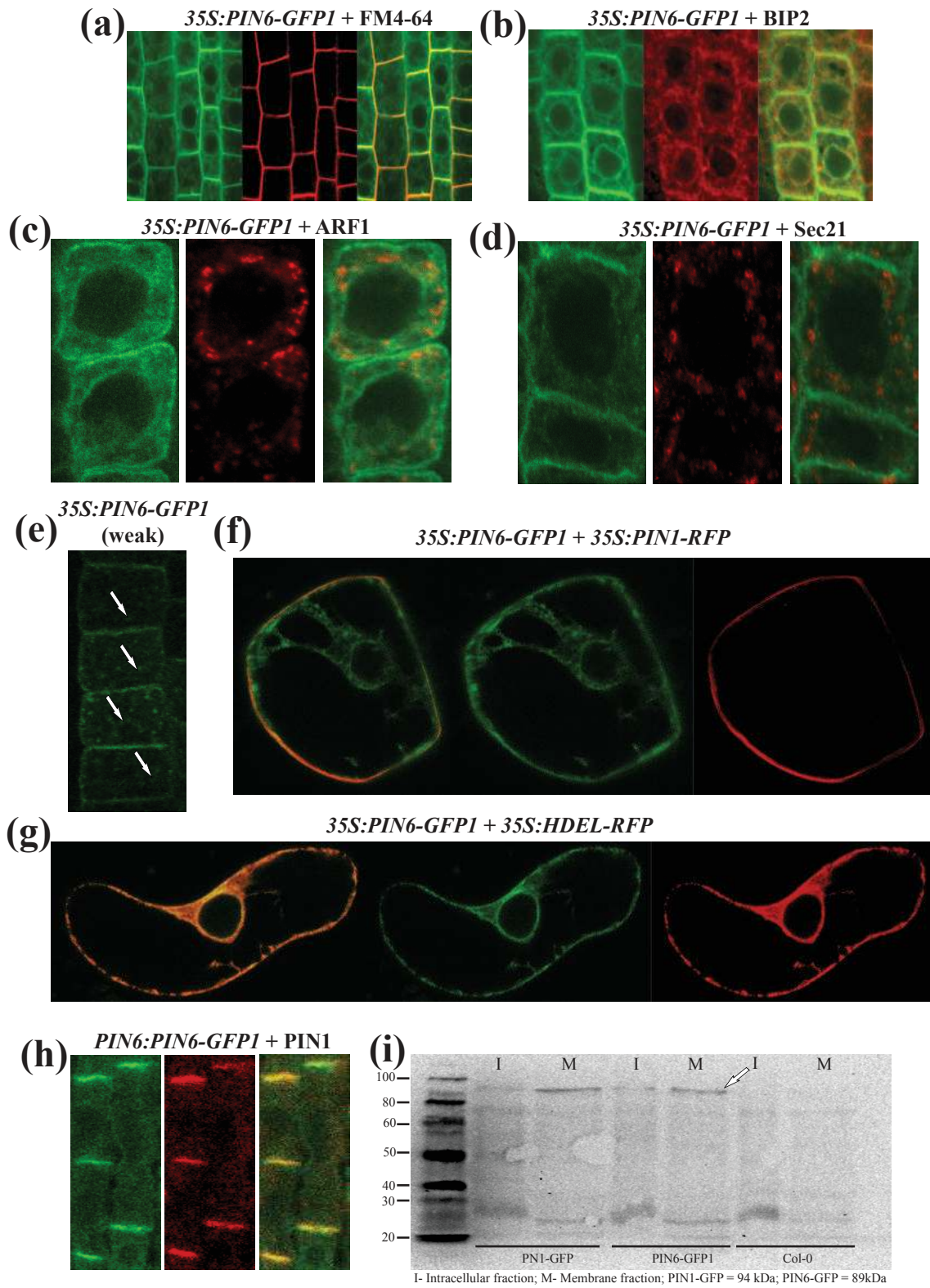I- Intracellular fraction; M- Membrane fraction; PIN1-GFP = 94 kDa; PIN6-GFP = 89kDa

Figure S4

PIN6:GUS

Root-shoot junction

Table S1 Primer sequences used for preparation of PIN6-GFP construct through overlap PCR

	Name	Sequence
35S:PIN6-GFP1	A R	5´-GCTCCTCGCCCTTGCTCACCAT ACCACCCGGAAACTCTG-3´
	B F	5´-CAGAGTTTCCGGGTGGT ATGGTGAGCAAGGGCGAGGAGCT-3´
	B R	5´-GATCCGGCTGCTTGACCACCACC CAGCTCGTCCATGCCGAGAG-3´
	C F	5´-CTCGGCATGGACGAGCTG GGTGGTCAAGCAGCCGGATCAATCG-3´
35S:PIN6-GFP2	A R	5´-CTCGCCCTTGCTC ACCATTCCTCCGCCGTGGGAGAAAC-3´
	B F	5´-GTTTCTTCCACGGCGGAGGA ATGGTGAGCAAGGGCGAG-3´
	B R	5´-GGTACCGCTTCCTCCTCC CAGCTCGTCCATGCCGAGAG-3´
	C F	5´-GATCACTCTCGGCATGGACGAGCTG GGAGGAGGAAGCGGTA CCCTTCAG-3´
35S:PIN6-GFP3	A R	5´-CTCGCCCTTGCTCACCAT ACCACCACCACCGGCTTTGAAG-3´
	B F	5´-TCTTCAAAGCCGGTGGTGGTGGT ATGGTGAGCAAGGGCGAGGAGCTG-3´
	B R	5´-GAGCCAATCGAGACCACCACC AGCTCGTCCATGCCGAGAGTC-3´
	C F	5´-CTCGGCATGGACGAGCTG GGTGGTGGTCTCGATTGGCTCAT-3´
PIN6 ATTB1 F		5´-GGGGACAAGTTTGTACAAAAAAGCAGGCTCG ATGATAACGGGAA ACGAATTCTAC-3´
PIN6 ATTB2 R		5´-GGGGACCACTTTGTACAAGAAAGCTGGTC TCATAGGCCCAAGAGG ACGTAG-3´

A, B and C are three different PCR product fragments. A and C are the two PIN6 fragments between this, fragment B is inserted which is the GFP fragment. Double spce included in each primer between the overlapping regions.